Keaton et. al Supplementary Materials

Results and Discussion

Cdc28p phosphorylation upon Swe1p overexpression

To induce a cell cycle arrest by overexpression of Swe1p, cells were grown in neutral sucrose-containing media and *GAL1-SWE1* expression was induced by the addition of 2% galactose. After 4 h the cells were uniformly arrested with elongated buds (due to the inability of Clb1,2p/Cdc28p to trigger the apical-to-isotropic growth switch [1]). Although overall Cdc28p Y19 phosphorylation was increased under these circumstances, we were surprised to find that Clb2p/Cdc28p complexes were phosphorylated to a low and somewhat variable stoichiometry (Fig. S3A). Indeed, the stoichiometry of phosphorylation associated with Clb2p/Cdc28p was reproducibly lower than the phosphorylation associated with Clb2p/Cdc28p in *hsl1*Δ cells (Fig. S3B). This unexpected result was confirmed by 2D gel analysis of Clb2p-associated Cdc28p, which migrated similarly to Y19-unphosphorylated Cdc28p from *swe1*Δ cells (Fig. S3D). In contrast, Clb5p-associated Cdc28p was significantly phosphorylated in cells arrested by Swe1p overexpression (Fig. S3A, D). These observations imply that overexpressed Swe1p behaves in an anomalous manner.

An unexpected finding from the 2D gel analysis was the presence of three species of Cdc28p in complexes purified from *swe1*Δ cells (Fig. S3D, spots 1-3). The only characterized modifications of Cdc28p are an activating phosphorylation at T169 and inhibitory phosphorylation at Y19 [2]. As all cyclin-bound Cdc28p is thought to be

phosphorylated at T169 [3] and no Y19 phosphorylation should occur in *swe1*Δ cells, we expected to detect a single species of Cdc28p. Dephosphorylation of T169 seems unlikely given prior studies [3]; thus, there appears to be at least one, and probably two, additional as-yet-uncharacterized modifications of Cdc28p that affect its net charge. Interestingly, Solomon and colleagues reported potentially similar modifications of the CDK Kin28p that were not due to phosphorylation but that affected the apparent net charge in 2D gel electrophoresis [4].

To assess phosphorylation in a cell cycle arrest mediated by endogenous Swe1p, we depleted Hsl7p from strains lacking Mih1p. Under these conditions, Clb2p and Clb5p complexes displayed similarly high levels of Cdc28p Y19 phosphorylation (Fig. S3C, D). Exact quantitation of the percentage of Y19 phosphorylation based on 2D gels was not possible because two of the Y19-phosphorylated spots detected in Cdc28p from cells lacking Mih1p and Hsl7p co-migrated with Y19-unphosphorylated spots detected in Cdc28p from *swe1*Δ cells (Fig. S3D, spots 2 and 3). In favorable gels a slight separation of spot 2 into two species was detectable (not shown), supporting the idea that both Y19-phosphorylated and Y19-unphosphorylated species (presumably differing in some other modification) co-migrate. Nevertheless, the spot pattern shifts markedly from predominantly spots 1 and 2 in *swe1*Δ cells to predominantly spots 3-5 in cells arrested by endogenous Swe1p. We estimate that Clb2p and Clb5p-associated Cdc28p is >80% phosphorylated under these conditions.

In previous studies, Swe1p overexpression was often used as a surrogate for physiological conditions that trigger a checkpoint resulting in Swe1p-mediated arrest [5-7]. Our data show that Swe1p overexpression yields a quite different Cdc28p

phosphorylation profile from that observed with physiological Swe1p levels. The simplest way to explain this phenotype is that unlike endogenously expressed Swe1p, overexpressed Swe1p binds to Clb2p/Cdc28p complexes and inhibits their activity without actually phosphorylating the Cdc28p. Consistent with this proposal, Swe1p has been shown to bind Clb2p/Cdc28p [8, 9] and Swe1p can mildly delay nuclear division even in cells containing a non-phosphorylatable mutant *CDC28* allele [7].

It is not clear why overexpressed Swe1p does not promote Clb2p/Cdc28p phosphorylation. We speculate that high-level expression swamps out folding or regulatory factors, creating a large pool of an aberrant form of Swe1p that can bind Clb2p/Cdc28p but lacks kinase activity. Binding of this inactive Swe1p then simultaneously inhibits the Clb2p/Cdc28p (causing cell cycle arrest) and protects it from phosphorylation by the smaller pool of active Swe1p. In the case of Clb5p/Cdc28p, the inactive Swe1p does not bind (or binds weakly), allowing access of active Swe1p and phosphorylation of the complex. One possible basis for the difference between active and inactive Swe1p pools is suggested by recent work arguing that Swe1p phosphorylation at multiple sites by Cdc28p is important for Swe1p kinase activity, but perhaps not for Clb2p/Cdc28p binding [9]. Our findings highlight the dangers of overexpression studies; we stress that all of our main conclusions stem from analysis of the *in vivo* phosphorylation state of Cdc28p under conditions where all cyclins, Swe1p, and Mih1p were expressed at endogenous levels.

Materials and Methods

Yeast strains and plasmids

All yeast strains used in this study are in the BF264-15DU background (*ade1, his2, leu2-3,112, trp1-1*^{a}*, ura3*Δ*ns*) [10] and are listed in Table 1. Standard genetic and molecular biology techniques were used for generation of all strains described here. The *swe1*::*LEU2* [5], *hsl1*::*URA3* [11], *mih1*::*LEU2* [12], *mih1*::TRP1 [13], *clb6*::*ADE1* [14], *clb5*::*ARG4* [15], *clb3*::*TRP1* and *clb4*::*HIS2* [16] disruptions have been described previously. The *GAL1-HSL7*:*LEU2* places the endogenous *HSL7* under control of the *GAL1* promoter, as described in [13].

The Spc42p-GFP construct, in which GFP is fused to the C-terminus of Spc42p and expressed from its own promoter, is an adaptation of pIA29 [17] with a KAN^{r} cassette inserted at *Not1* (gift from Steve Haase, Biology Department, Duke University). The plasmid was digested with *Stu1* to target integration by homologous recombination. The *GAL1-SWE1-12myc*:*LEU2* construct was generated by cloning a *BamHI*/*SacI* fragment from pJM1101 (*GAL1-SWE1-12myc*:*URA3*) [8] into the corresponding sites in pRS305 [18]. The resulting plasmid was digested at the unique *AflII* site to target integration at the *LEU2* locus. A plasmid containing *GAL1-SIC1*$^{\Delta 4p}$ (in which Sic1p residues T2, T5, T33, and S76 were mutated to alanine [19]) in pRS306 [18] was digested at the unique *Stu1* site to target integration at the *URA3* locus.

Cyclin-TAP alleles were previously described as part of the whole-genome yeast TAP-tagging collection [20]. The entire cyclin-TAP alleles, spanning from 200 bp upstream of the start codon to 200 bp downstream of the stop codon and including the

HIS3 marker, were amplified by PCR using genomic DNA from the published strains as template and the following primer pairs: CLN1, GCACACTTAAGAGCAAATTGGC and GCGTCATCTTTTCCGTTCATG; CLN2, GTAACTATTATGCTCCTCTTACTG and GATTAGACTTGAGTGCCATCAGC; CLB1, GCAGGCTGCAATTTTAGTGTC and CTTAAATATCATCGATAGACATAC; CLB2, TGACATAGAATATCTGTTGAAG and ATGGTGTGGTGTTATTAGTGAG; CLB3, GCGACAAGCGAAGGAACAAAAC and GAATGAGTTGTTTTGTTAACCTTG; CLB4, CCTAAAGTTATGCCTGCCCTATC and GATTCGGTCAAAAAGAGGATG; CLB5, CGGTTTATTAGAAGCTACTTGG and GATAATAGTAGTAATACTGGTGG. PCR products were transformed into JMY1-12 (*ura3 leu2 trp1 his3 ade1)* [21]. Integration (selected by histidine prototrophy) at the correct loci was confirmed by PCR or Western blot analysis.

swe1 temperature-sensitive alleles were generated by mutagenizing the *SWE1-12myc* plasmid pJM1062 [8] by serial passage through XL1-Red mutagenic *E. coli* (Strategene) for three days. The resulting DNA was transformed into DLY6286 (*swe1*Δ *hsl1*Δ *mih1*Δ) and transformed colonies were grown at 37°C and replica-plated to 24°C. Plasmids were recovered from transformants that grew at 37°C but arrested at 24°C with an elongated bud morphology and sequenced. The *swe1-12* allele was selected for further characterization based on a tight arrest at 24°C but no detectable Cdc28p Y19 phosphorylation at 37°C; it contained a single point mutation (E792Q) in a conserved C-terminal region of Swe1p. The entire gene (with myc tags) was subcloned into pRS304 with *BamH1/Xho1* to generate DLB2852. The plasmid was digested with *Bsu36I* to

target integration at the *TRP1* locus of DLY7748 and DLY7777. Transformants were screened by Western blot analysis for equal expression of Swe1-12p.

Media, growth conditions, and cell synchrony

Strains were grown in YEP (1% yeast extract 2% Bacto Peptone, 0.012% adenine, 0.01% uracil) media containing 2% dextrose (YEPD), sucrose (YEPS) or galactose (YEPG) at 30°C. *GAL1-SWE1-12myc* strains were grown in YEPS to 0.5 x10^7 cells/ml and Swe1p expression was induced by the addition of 2% galactose for 4 h. Cell cycle arrest by depletion of Hsl7p was achieved by growing *GAL1-HSL7 mih1*Δ in YEPD for 22 h. Strains containing *swe1-12* were grown at 37°C and arrested by the addition of hydroxyurea (Sigma) to a final concentration of 0.2 M for 5 hours. Cells were then shifted to 24°C by addition of ice-cold media containing hydroxyurea.

For pheromone arrest-release experiments, cells (1-2 x10^7 cells/ml) were incubated with 40 ng/ml α-factor for 2.5 h, then collected and resuspended in fresh media at 2.0 x10^7 cells/ml. A portion of the culture was treated with 150 μM Latrunculin B (BioMol Research Laboratories Inc) just prior to budding (LAT treatment immediately following pheromone removal prevents release from the G1 arrest [22]). Cells were either fixed in 70% ethanol overnight for FACS analysis or 4% paraformaldehyde in Solution B (100 mM $KHPO_4$ pH7.5, 1.2 M sorbitol [23]) for 5 min. Paraformaldehyde-fixed samples were rinsed in Solution B twice and resuspended in mounting media (90% glycerol, 9.2 mM p-phenylenediamine, 3 μM DAPI [4'6'-diamidino-2-phenylindole]) [23] to score SPB separation, budding, and nuclear division. At least 200 cells were scored for each sample.

For synchronization of strains containing *GAL1-SIC1*$^{\Delta 4p}$, cells were grown in YEPS and arrested with 40 ng/ml α-factor for 4 h. Sic1$^{\Delta 4p}$ expression was induced 30 min prior to release by the addition of 2% galactose, after which, cells were collected and resuspended in YEPG to release them from G1 arrest.

For synchronization by centrifugal elutriation, cells were grown in YEPG to $2x10^7$ cells/ml and 2% dextrose was added 30 min prior to elutriation, which was then performed as described in [1]. G1 daughter cells were resuspended in warm YEPD to $2x10^7$ cells/ml.

FACS analysis and Microscopy

Cell preparation for FACS analysis was performed as previously described [24]. Cells were fixed overnight in 70% ethanol, washed in H_2O, and incubated in 2 mg/ml RNAse A (Sigma) in 50 mM Tris-HCl pH 8.0 overnight at 37°C. Cells were then treated with 5 mg/ml pepsin (Sigma) in 0.45% HCl (vol/vol) for 15 min prior to DNA staining with Sytox Green (Invitrogen) in 50 mM Tris-HCl pH 7.5. DNA content of 10,000 nuclei was measured using a Becton Dickinson FACScan and analyzed using CellQuest software (Becton Dickinson Immunocytometry Systems).

For microscopy, paraformaldehyde or ethanol fixed samples were washed in Solution B or phosphate-buffered saline, sonicated, and DNA was stained with 1 μM DAPI. DIC and fluorescent images were acquired with an 100X objective on a Zeiss Axioimager microscope with a Hamamatsu Orca ER monochrome cooled-CCD camera and processed using MetaMorph (Universal Imaging Corp) and Photoshop (Adobe) software.

Yeast lysates, TAP isolation, and immunoblotting

Cells grown to mid-log phase were harvested by centrifugation and pellets were stored at -80°C. Yeast pellets were resuspended in TAP-lysis buffer (20 mM HEPES pH 7.5, 300 mM NaCl, 1 mM $MgCl_2$, 2 mM $CaCl_2$, 0.1% Tween-20, 1 mM β-mercaptoethanol, 1 mM Na_3VO_4, 1 μg/ml leupeptin, 1 μg/ml pepstatin, 1.5 μg/ml aprotinin, 1 mM benzamidine, 1 mM PMSF). Acid-washed glass beads and 2 μl of AntifoamA (Sigma) were added before homogenization in a BeadBeater (BioSpec Products) for 1.5 min. Lysates were clarified by centrifugation at 13,000 rpm in a Biofuge microcentrifuge for 15 min at 4°C and protein concentration was determined using Bradford assay (BioRad).

For purification of cyclin-TAP complexes, various amounts of lysate from asynchronous cells were used to isolate approximately equal amounts of associated Cdc28p (8 mg for Cln1p-TAP and Cln2p-TAP, 2 mg for Clb2p-TAP, 4 mg for Clb3p-TAP, 6 mg for Clb4p-TAP, and 15 mg for Clb5p-TAP due to Clb5p proteolysis after lysis). Lysates were diluted to 10 mg/ml protein in TAP-lysis buffer and incubated for 1 hr at 4°C with 25-50 μl of a 50% slurry of calmodulin affinity resin (Stratagene) that had been blocked in 1% ovalbumin (Sigma) in TAP-lysis buffer. Cyclin-TAP complexes bound to the calmodulin resin were washed several times with TAP-lysis buffer and eluted in 50 μl elution buffer (50 mM Tris-HCl pH 8.0, 5 mM EGTA).

For immunoblotting, eluted cyclin-TAP complexes or 100 μg of clarified lysate were mixed with 4X sample loading buffer (30 mM Tris-HCl, pH 6.8. 0.5% SDS, 12.5% glycerol, 175 mM β-mercaptoethanol, 0.005% bromophenol blue, final concentration) and heated at 95°C for 5 min prior to separation on a 10% SDS-PAGE gel. Proteins were

then transferred to nitrocellulose (Pall Corporation), blocked in a 1:1 solution of Odyssey Blocking Buffer (LI-COR Biosciences) and TBS (50 mM Tris-HCl, pH 7.6, 150 mM NaCl), and incubated in primary antibodies diluted in blocking buffer containing 0.1% Tween-20 overnight. Blots were stained with antibodies against total Cdc28p (1:10,000 mouse anti-PSTAIRE) and tyrosine phosphorylated Cdc28p (1:2,000 rabbit anti-phosho-Cdc2(Tyr15), Cell Signaling Technology) or against the TAP-tag (1:2,000 rabbit anti-calmodulin binding protein epitope tag, Upstate Cell Signaling Solutions). After several washes in TBS with 0.1% Tween-20, blots were incubated with fluorescent goat anti-mouse IRdye800 and goat anti-rabbit AlexaFlour680 secondary antibodies (1:7,500, Molecular Probes) in blocking buffer with 0.1% Tween-20 and 0.01% SDS for 1 h at room temperature. Membranes were scanned using an Odyssey scanner and integrated fluorescence was quantitated using Odyssey software (LiCor).

For the blot in Fig. 6B, proteins were isolated by TCA precipitation. Approximately $1x10^7$ cells were collected and resuspended in pronase buffer (25 mM Tris-HCl, pH 7.5, 1.4 M Sorbitol, 20 mM NaN_3, 2 mM $MgCl_2$). Trichloroacetic acid (TCA 100% w/v, Sigma) was added to a final concentration of 17% v/v and cell suspensions were stored at -80°C. Samples were thawed and cells were homogenized by addition of glass beads (Sigma) and vortexing at 4°C for 10 min. The lysate was collected and the beads were washed 2X with 5% w/v TCA to recover the remaining lysate. Precipitated proteins were collected by centrifugation in a Biofuge microcentrifuge for 15 min at 4°C. Pellets were then resuspended in Thorner sample buffer (40 mM Tris-HCl, Ph 6.8, 8 M Urea, 5% SDS, 143 mM β-mercaptoethanol, 0.1

mM EDTA, 0.4 mg/ml Bromophenol Blue) and any residual TCA was neutralized by the addition of 2M Tris-HCl pH 8.0.

2D Gel electrophoresis

Salt and detergent were removed from the eluted Clb-TAP/Cdc28p complexes using a TCA-like precipitation procedure (ReadyPrep 2D cleanup kit, Bio-Rad). Purified samples were resuspended in 200 µl of rehydration buffer (8.5 M urea, 4% 3-[(3-Cholamidopropyl)dimethylammonio]-1-propanesulfonate, 2 mM tributyl phosphine, and 0.2% pH 3-10 carrier ampholyte), applied to ReadyStrip IPG strips (11 cm; pH 3-10; Bio-Rad), and actively rehydrated at 50 V for 12 h at 20°C. Samples were focused at 250 V for 20 min, gradually ramped up to 8000 V for 2.5 h, and maintained at 8000 V for a total of 35000 V-h per gel. Focused strips were either processed immediately for second dimensional analysis or stored at –80°C. Focused ReadyStrips were then incubated in 2.5 ml of equilibration buffer (6 M urea, 2% SDS, 50 mM Tris-HCl pH 8.8, and 20% glycerol) with 2% DTT for 20 min with agitation, followed by a 20 min incubation in equilibration buffer with 2.5% iodoacetamide. Equilibrated strips were rinsed in Tris-glycine SDS running buffer, inserted into the IPG well of a 15% Tris-HCl Criterion Gel (Bio-Rad), and covered with low-melting point agarose (0.5%). Gels were run at 200 V for 60 min and prepared for Western transfer and immunoblotting as described above.

Histone H1 Kinase Assays

Cell lysates were prepared and the purification of Clb2p-TAP and Clb5p-TAP complexes were performed as above using calmodulin affinity resin. Beads were washed

once with TAP-lysis buffer, 3X with RIPA buffer supplemented with $MgCl_2$ and $CaCl_2$ (50 mM Tris-HCl pH 7.5, 120 mM NaCl, 1% deoxycholate, 1% Triton X-100, 0.1% SDS, 1 mM $MgCl_2$, 2 mM $CaCl_2$), and once with Tris/Mg/Ca buffer (50 mM Tris-HCl, pH 7.5, 1 mM $MgCl_2$, 2 mM $CaCl_2$). Bead-bound complexes were divided into two, resuspended in phosphatase buffer (50 mM Tris-HCl pH 6.8, 50 mM NaCl, 1 mM DTT, 1 mM EDTA, 4 mM $CaCl_2$, 2 mM $MgCl_2$), and treated with or without 2 μl of purified human Cdc25C for 20 min at room temperature. The catalytic domain of hCdc25C was expressed as an untagged protein in *E. coli* as previously described [25]. Beads were then washed with Tris/Mg/Ca buffer and eluted in 50 mM Tris-HCl pH 8.0, 5 mM EGTA. 50 μl of eluate was used for immunoblotting. Equal amounts of eluate (5 μl) were used in triplicate kinase assay reactions consisting of 10 mM Tris-HCl pH 7.5, 12.5 mM $MgCl_2$, 15 μg of histone H1 (Sigma), 10 μM ATP (Sigma), and 2.5 μCi [γ-^{32}P]-ATP (Perkin Elmer). Reactions were carried out at 30°C for the indicated times and stopped by the addition of sample buffer and heating at 95°C for 5 min. Samples were run on a 12.5% SDS-PAGE and the gel was boiled in 5% TCA for 15 min prior to drying and exposure to a phosphoimager cassette. The relative ^{32}P incorporation was determined using a STORM 840 scanner (Amersham Biosciences) and ImageQuant software (version 5.2, Molecular Dynamics).

Wee1 kinase assay

The human Cyclin A/Cdk2 complex, in which Cyclin A is truncated and encompasses residues 174-432, was prepared as previously described [26, 27]. Recombinant Wee1 from *Xenopus laevis* was expressed as a GST-tagged protein in *E.*

coli and purified as described previously [28]. Human $p27^{Kip1}$ was expressed as a His-tagged protein in *E. coli* and purified as previously described [29]. Protein concentrations were determined by Bradford assay. Given the tight affinity of $p27^{Kip1}$ for cyclin/CDK complexes (≤ 10 nM) [29], we expected that one equivalent of $p27^{Kip1}$ would be sufficient to form a stoichiometric complex under our reaction conditions (~200 nM). Phosphorylation reactions were performed for 10 min at room temperature in 50 mM Tris-HCl pH 7.5, 50 mM NaCl, 10 mM $MgCl_2$, and 1 mM DTT with 2 mM [γ-^{32}P]-ATP (200-500 Ci/mol, Perkin-Elmer), 0.3 μM Cdk2/Cyclin A and 0.2 μM Wee1. Reactions were quenched by the addition of Laemmli buffer and phosphorylation was visualized by autoradiography following SDS-PAGE.

Table 1. Yeast strains used in this study.

DLY1	MAT**a** *bar1*
DLY1028	MAT**a** *bar1 swe1::LEU2*
DLY2707	MAT**a** *bar1 mih1::LEU2*
DLY6286	MATα *swe1::LEU2 mih1::LEU2 hsl1::TRP1*
DLY7598	MAT**a** *bar1 CLB2-TAP:HIS3 his3 HIS2*
DLY7599	MAT**a** *bar1 CLB4-TAP:HIS3 his3 HIS2*
DLY7646	MAT**a** *bar1 CLN1-TAP:HIS3 his3 HIS2*
DLY7647	MAT**a** *bar1 CLN2-TAP:HIS3 his3 HIS2*
DLY7648	MAT**a** *bar1 CLB3-TAP:HIS3 his3 HIS2*
DLY7649	MAT**a** *bar1 CLB1-TAP:HIS3 his3 HIS2*
DLY7662	MAT**a** *bar1 CLB5-TAP:HIS3 his3 HIS2*
DLY7711	MAT**a** *CLB2-TAP:HIS3 hsl1::URA3*
DLY7712	MAT**a** *bar1 CLB2-TAP:HIS3 swe1::LEU2 mih1::LEU2*
DLY7717	MAT**a** *CLN2-TAP:HIS3 mih1::LEU2*
DLY7718	MATα *CLN2-TAP:HIS3 hsl1::URA3*
DLY7735	MAT**a** *CLN1-TAP:HIS3 hsl1::URA3*
DLY7748	MAT**a** *CLB5-TAP:HIS3 swe1::LEU2 mih1::LEU2 hsl1::URA3*
DLY7749	MAT**a** *CLB5-TAP:HIS3 hsl1::URA3*
DLY7770	MAT**a** *CLB4-TAP:HIS3 hsl1::URA3*
DLY7777	MATα *CLB2-TAP:HIS3 swe1::LEU2 mih1::LEU2 hsl1::URA3*
DLY7786	MAT**a** *CLB5-TAP:HIS3 mih1::LEU2*
DLY7799	MAT**a** *bar1 CLN1-TAP:HIS3 GAL1-SWE1-12myc:LEU2 his3 HIS2*
DLY7802	MAT**a** *bar1 CLN2-TAP:HIS3 GAL1-SWE1-12myc:LEU2 his3 HIS2*
DLY7808	MAT**a** *bar1 CLB2-TAP:HIS3 GAL1-SWE1-12myc:LEU2 his3 HIS2*
DLY7811	MAT**a** *bar1 CLB3-TAP:HIS3 GAL1-SWE1-12myc:LEU2 his3 HIS2*
DLY7814	MAT**a** *bar1 CLB4-TAP:HIS3 GAL1-SWE1-12myc:LEU2 his3 HIS2*
DLY7817	MAT**a** *bar1 CLB5-TAP:HIS3 GAL1-SWE1-12myc:LEU2 his3 HIS2*
DLY7854	MATα *CLB2-TAP:HIS3 mih1::LEU2*
DLY7857	MATα *CLN1-TAP:HIS3 mih1::LEU2*
DLY7858	MAT**a** *CLB3-TAP:HIS3 mih1::LEU2*
DLY7860	MAT**a** *CLB4-TAP:HIS3 mih1::LEU2*
DLY7873	MAT**a** *CLB3-TAP:HIS3 hsl1::URA3*
DLY7944	MAT**a** *CLB2-TAP:HIS3 hsl1::URA3*
DLY7946	MAT**a** *CLB2-TAP:HIS3 GAL1-SWE1-12myc:LEU2*
DLY7974	MAT**a** *bar1 SPC42-GFP:TRP1,KAN^{r}*
DLY8197	MAT**a** *hsl7::GAL1-HSL7:LEU2 mih1::TRP CLB2-TAP:HIS3*
DLY8199	MAT**a** *hsl7::GAL1-HSL7:LEU2 mih1::TRP CLB5-TAP:HIS3*
DLY8245	MAT**a** *bar1 clb6::ADE1 SPC42-GFP:TRP1,KAN^{r}*
DLY8261	MAT**a** *bar1 clb6::ADE1 SPC42-GFP:TRP1,KAN^{r} swe1::LEU2*
DLY8297	MAT**a** *bar1 SPC42-GFP:TRP1,KAN^{r} clb3::TRP1, clb4::HIS2*
DLY8300	MAT**a** *bar1 clb5::ARG4 clb6::ADE1 SPC42-GFP:TRP1,KAN^{r}*
DLY8441	MAT**a** *bar1 clb6::ADE1 SPC42-GFP:TRP1,KAN^{r} mih1::LEU2*
DLY8700	MAT**a** *bar1 CLB5-TAP:HIS3 mih1::LEU2 GAL1-SIC1$^{\Delta 4p}$-HA:URA3*
DLY8701	MAT**a** *bar1 CLB5-TAP:HIS3 mih1::LEU2 URA3*

DLY8726	MAT**a** *bar1 CLB2-TAP:HIS3, swe1:LEU2, hsl1:URA3, mih1:LEU2, swe1-12-12myc:TRP1*
DLY8727	MAT**a** *CLB5-TAP:HIS3, swe1:LEU2, hsl1:URA3, mih1:LEU2, swe1-12-12myc:TRP1*
DLY8736	MAT**a** *bar1 SPC42-GFP:TRP1,KAN^r swe1::LEU2*
DLY8963	MAT**a** *bar1 clb5::ARG4 clb6::ADE1 swe1::LEU2 SPC42-GFP:TRP1,KAN^r*
JMY1-12	MAT**a** *bar1 ura3 leu2 trp1 his3 ade1*

Figure Legends

Figure S1. Synchrony and Swe1p-dependence controls for Fig. 1. A-C) As a control for the synchrony experiment of Fig. 1A-C, *swe1*Δ (DLY8736) cells were synchronized by pheremone arrest/release and treated with LAT at 21 min (just prior to budding). A) Budding (circles) and nuclear division (squares) were scored, showing that in this case, nuclear division proceeded after a brief delay even in the presence of LAT. This delay is likely due to LAT toxicity. B) FACS profiles for untreated (black) and LAT-treated (red) samples during (30 min) and after (40 min) S phase. As with the wild-type, DNA replication timing is unaffected by LAT in *swe1*Δ mutants. C) Spindle formation was monitored by fluorescence microscopy to visualize the SPB marker Spc42-GFP, and >200 cells were scored for each sample. D-G) Cells lacking specific pairs of related cyclins were synchronized and treated with LAT as above. D) Budding (circles) and nuclear division (squares) in *clb5*Δ *clb6*Δ (DLY8300) and *clb5*Δ *clb6*Δ *swe1*Δ (DLY8963) cells. E) DNA replication profiles from the same experiment. F) FACS profile overlays of untreated and LAT-treated samples for the same experiment at 120 min following release from G1 arrest. At this time even the *clb5*Δ *clb6*Δ cells have started to increase their DNA content. It is unclear whether this delayed replication is due to Clb1,2p, Clb3,4p, or Cln1-3p complexes that might accumulate during the delay.

G) Budding, spindle formation, and nuclear division in WT (DLY8245) and *clb3*Δ *clb4*Δ (DLY8297) cells containing Spc42p-GFP. >200 cells were scored for each sample. H) WT (DLY8245) and *clb3*Δ *clb4*Δ (DLY8297) cells synchronized as above were scored for SPB separation after 3 h of LAT treatment. Unlike the DNA replication block in *clb5*Δ *clb6*Δ cells (above), the SPB separation block in *clb3*Δ *clb4*Δ cells was not leaky within this timeframe.

Figure S2. LAT does not block DNA replication in cells synchronized by centrifugal elutriation. Small G1 daughter cells were isolated from proliferating populations of WT (DLY1), *swe1*Δ (DLY1028), and *mih1*Δ (DLY2707) strains by centrifugal elutriation as described in Materials and Methods. The synchronized cells were inoculated into fresh YEPD at 30°C and 150 μM LAT was added to part of the culture at 15 min. Samples taken at the indicated times were processed for FACS analysis as described in Materials and Methods, and scored for budding (A), nuclear division (B), and DNA replication (C). The *swe1*Δ population was slightly delayed relative to the others (A), presumably because of a smaller starting cell size. LAT blocked nuclear division except in *swe1*Δ cells (B). DNA replication proceeded with similar timing in all strains (C), with a slight delay in *swe1*Δ cells as expected from their delayed budding (A). Because LAT slows cell growth [30], DNA replication was delayed in all strains relative to untreated cells (not shown).

Figure S3. Overexpressed Swe1p leads to cell cycle arrest with little phosphorylation of Clb2p/Cdc28p complexes. A) *GAL1-SWE1-12myc* cells

(DLY7799, DLY7802, DLY7808, DLY7811, DLY7814, DLY7817) were grown in sucrose-containing media and induced to overexpress Swe1p by addition of galactose for 4 h. Cdc28p Y19 phosphorylation was assessed for Cyclin-TAP/Cdc28p complexes from arrested cells. B) Comparison of Clb2p/Cdc28p phosphorylation in proliferating *hsl1*Δ (DLY7944) and arrested *GAL-SWE1-12myc* (DLY7946) cells. C) *mih1Δ GAL1-HSL7* cells (DLY8197 and DLY8199) were grown in glucose-containing medium for 22 h to deplete Hsl7p leading to Swe1p-mediated arrest (*mih1*Δ *hsl7-OFF*). Cdc28p Y19 phosphorylation was assessed for Cyclin-TAP/Cdc28p complexes from arrested cells. D) Clb2p/Cdc28p and Clb5p/Cdc28p complexes were isolated from proliferating *swe1*Δ cells (DLY7712 and DLY7748), arrested *GAL1-SWE1-12myc* cells (DLY7946 and DLY7817 induced to overexpress Swe1p), and arrested *mih1*Δ *GAL1-HSL7* cells (DLY8197 and DLY8199 repressed to deplete Hsl7p) and subjected to 2D electrophoresis and Western blot analysis. Spots are numbered according to migration from basic to acidic in the first dimension. (red, pY19; green, total Cdc28p)

Supplemental References

1. Lew, D.J., and Reed, S.I. (1993). Morphogenesis in the yeast cell cycle: regulation by Cdc28 and cyclins. J. Cell Biol. *120*, 1305-1320.
2. Morgan, D.O. (1995). Principles of CDK regulation. Nature *374*, 131-134.
3. Cheng, A., Ross, K.E., Kaldis, P., and Solomon, M.J. (1999). Dephosphorylation of cyclin-dependent kinases by type 2C protein phosphatases. Genes Dev. *13*, 2946-2957.
4. Kimmelman, J., Kaldis, P., Hengartner, C.J., Laff, G.M., Koh, S.S., Young, R.A., and Solomon, M.J. (1999). Activating phosphorylation of the Kin28p subunit of yeast TFIIH by Cak1p. Mol. Cell. Biol. *19*, 4774-4787.
5. Booher, R.N., Deshaies, R.J., and Kirschner, M.W. (1993). Properties of Saccharomyces cerevisiae wee1 and its differential regulation of p34CDC28 in response to G1 and G2 cyclins. EMBO J. *12*, 3417-3426.

6. Lim, H.H., Goh, P.Y., and Surana, U. (1996). Spindle pole body separation in Saccharomyces cerevisiae requires dephosphorylation of the tyrosine 19 residue of Cdc28. Mol. Cell. Biol. *16*, 6385-6397.
7. McMillan, J.N., Sia, R.A., Bardes, E.S., and Lew, D.J. (1999). Phosphorylation-independent inhibition of Cdc28p by the tyrosine kinase Swe1p in the morphogenesis checkpoint. Mol. Cell. Biol. *19*, 5981-5990.
8. McMillan, J.N., Theesfeld, C.L., Harrison, J.C., Bardes, E.S., and Lew, D.J. (2002). Determinants of Swe1p degradation in Saccharomyces cerevisiae. Mol. Biol. Cell. *13*, 3560-3575.
9. Harvey, S.L., Charlet, A., Haas, W., Gygi, S.P., and Kellogg, D.R. (2005). Cdk1-dependent regulation of the mitotic inhibitor Wee1. Cell *122*, 407-420.
10. Richardson, H.E., Wittenberg, C., Cross, F., and Reed, S.I. (1989). An essential G1 function for cyclin-like proteins in yeast. Cell *59*, 1127-1133.
11. Ma, X.J., Lu, Q., and Grunstein, M. (1996). A search for proteins that interact genetically with histone H3 and H4 amino termini uncovers novel regulators of the Swe1 kinase in Saccharomyces cerevisiae. Genes Dev. *10*, 1327-1340.
12. Russell, P., Moreno, S., and Reed, S.I. (1989). Conservation of mitotic controls in fission and budding yeasts. Cell *57*, 295-303.
13. McMillan, J.N., Longtine, M.S., Sia, R.A., Theesfeld, C.L., Bardes, E.S., Pringle, J.R., and Lew, D.J. (1999). The morphogenesis checkpoint in Saccharomyces cerevisiae: cell cycle control of Swe1p degradation by Hsl1p and Hsl7p. Mol. Cell. Biol. *19*, 6929-6939.
14. Basco, R.D., Segal, M.D., and Reed, S.I. (1995). Negative regulation of G1 and G2 by S-phase cyclins of Saccharomyces cerevisiae. Mol. Cell. Biol. *15*, 5030-5042.
15. Epstein, C.B., and Cross, F.R. (1992). CLB5: a novel B cyclin from budding yeast with a role in S phase. Genes Dev. *6*, 1695-1706.
16. Richardson, H., Lew, D.J., Henze, M., Sugimoto, K., and Reed, S.I. (1992). Cyclin-B homologs in Saccharomyces cerevisiae function in S phase and in G2. Genes Dev. *6*, 2021-2034.
17. Adams, I.R., and Kilmartin, J.V. (1999). Localization of core spindle pole body (SPB) components during SPB duplication in Saccharomyces cerevisiae. J. Cell. Biol. *145*, 809-823.
18. Sikorski, R.S., and Hieter, P. (1989). A system of shuttle vectors and yeast host strains designed for efficient manipulation of DNA in Saccharomyces cerevisiae. Genetics *122*, 19-27.
19. Verma, R., Annan, R.S., Huddleston, M.J., Carr, S.A., Reynard, G., and Deshaies, R.J. (1997). Phosphorylation of Sic1p by G1 Cdk required for its degradation and entry into S phase. Science *278*, 455-460.
20. Ghaemmaghami, S., Huh, W.K., Bower, K., Howson, R.W., Belle, A., Dephoure, N., O'Shea, E.K., and Weissman, J.S. (2003). Global analysis of protein expression in yeast. Nature *425*, 737-741.
21. Bose, I., Irazoqui, J.E., Moskow, J.J., Bardes, E.S., Zyla, T.R., and Lew, D.J. (2001). Assembly of scaffold-mediated complexes containing Cdc42p, the exchange factor Cdc24p, and the effector Cla4p required for cell cycle-regulated phosphorylation of Cdc24p. J. Biol. Chem. *276*, 7176-7186.

22. Theesfeld, C.L., Zyla, T.R., Bardes, E.G., and Lew, D.J. (2003). A monitor for bud emergence in the yeast morphogenesis checkpoint. Mol. Biol. Cell *14*, 3280-3291.
23. Pringle, J.R., Adams, A.E., Drubin, D.G., and Haarer, B.K. (1991). Immunofluorescence methods for yeast. Methods Enzymol. *194*, 565-602.
24. McNulty, J.J., and Lew, D.J. (2005). Swe1p responds to cytoskeletal perturbation, not bud size, in S. cerevisiae. Curr. Biol. *15*, 2190-2198.
25. Wilborn, M., Free, S., Ban, A., and Rudolph, J. (2001). The C-terminal tail of the dual-specificity Cdc25B phosphatase mediates modular substrate recognition. Biochemistry *40*, 14200-14206.
26. Jeffrey, P.D., Russo, A.A., Polyak, K., Gibbs, E., Hurwitz, J., Massague, J., and Pavletich, N.P. (1995). Mechanism of CDK activation revealed by the structure of a cyclinA-CDK2 complex. Nature *376*, 313-320.
27. Sohn, J., Parks, J.M., Buhrman, G., Brown, P., Kristjansdottir, K., Safi, A., Edelsbrunner, H., Yang, W., and Rudolph, J. (2005). Experimental validation of the docking orientation of Cdc25 with its Cdk2-CycA protein substrate. Biochemistry *44*, 16563-16573.
28. Kristjansdottir, K., and Rudolph, J. (2003). A fluorescence polarization assay for native protein substrates of kinases. Anal. Biochem. *316*, 41-49.
29. Xu, X., Nakano, T., Wick, S., Dubay, M., and Brizuela, L. (1999). Mechanism of Cdk2/Cyclin E inhibition by p27 and p27 phosphorylation. Biochemistry *38*, 8713-8722.
30. Karpova, T.S., Reck-Peterson, S.L., Elkind, N.B., Mooseker, M.S., Novick, P.J., and Cooper, J.A. (2000). Role of actin and Myo2p in polarized secretion and growth of Saccharomyces cerevisiae. Mol. Biol. Cell *11*, 1727-1737.

Figure S1

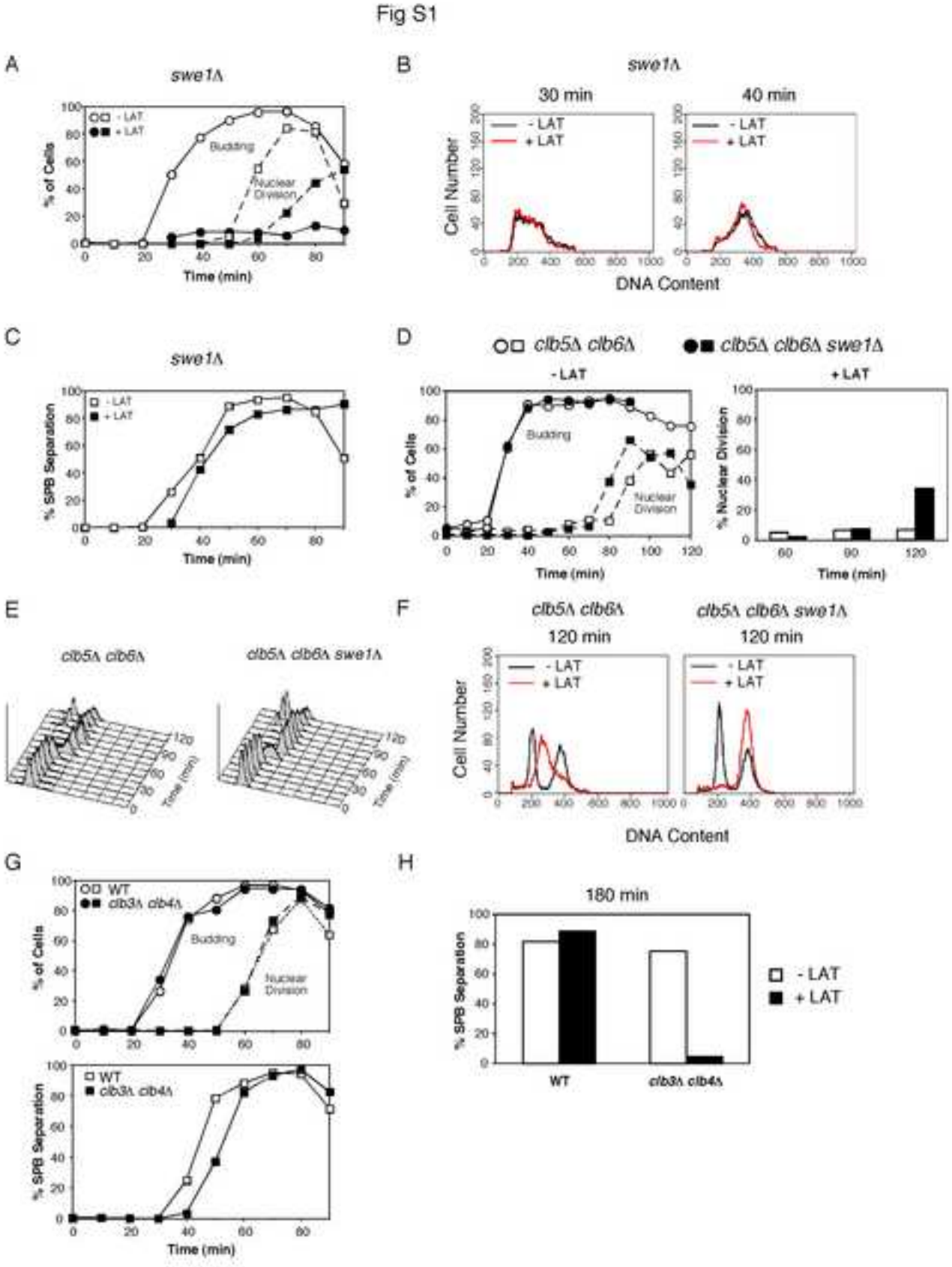
Fig S1
A
swe1Δ
- LAT
+ LAT
Budding
Nuclear Division
% of Cells
Time (min)
B
swe1Δ
30 min
40 min
- LAT
+ LAT
Cell Number
DNA Content
C
swe1Δ
- LAT
+ LAT
% SPB Separation
Time (min)
D
clb5Δ clb6Δ
clb5Δ clb6Δ swe1Δ
- LAT
+ LAT
Budding
Nuclear Division
% of Cells
% Nuclear Division
Time (min)
E
clb5Δ clb6Δ
clb5Δ clb6Δ swe1Δ
Time (min)
F
clb5Δ clb6Δ
clb5Δ clb6Δ swe1Δ
120 min
120 min
- LAT
+ LAT
Cell Number
DNA Content
G
WT
clb3Δ clb4Δ
Budding
Nuclear Division
% of Cells
% SPB Separation
Time (min)
H
180 min
% SPB Separation
- LAT
+ LAT
WT
clb3Δ clb4Δ

Figure S2

Fig S2

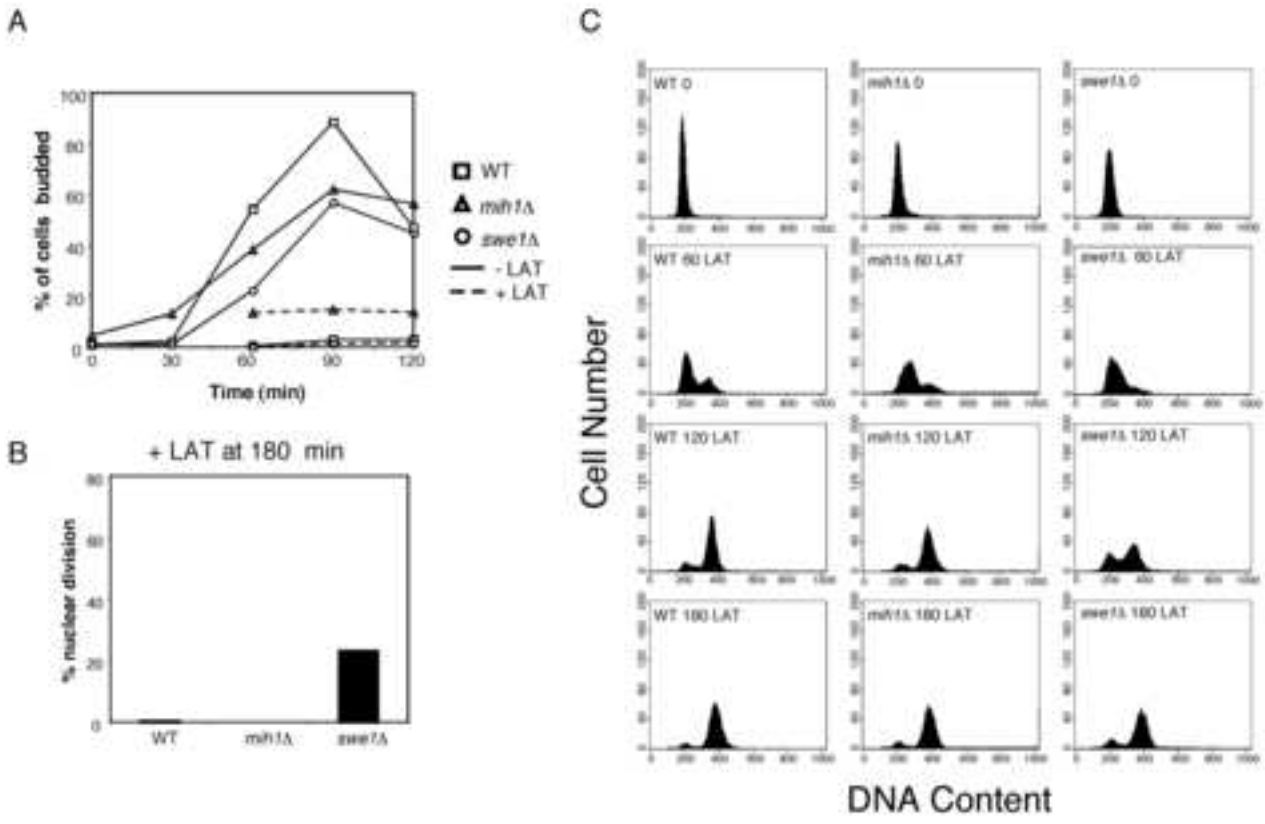

Figure S3

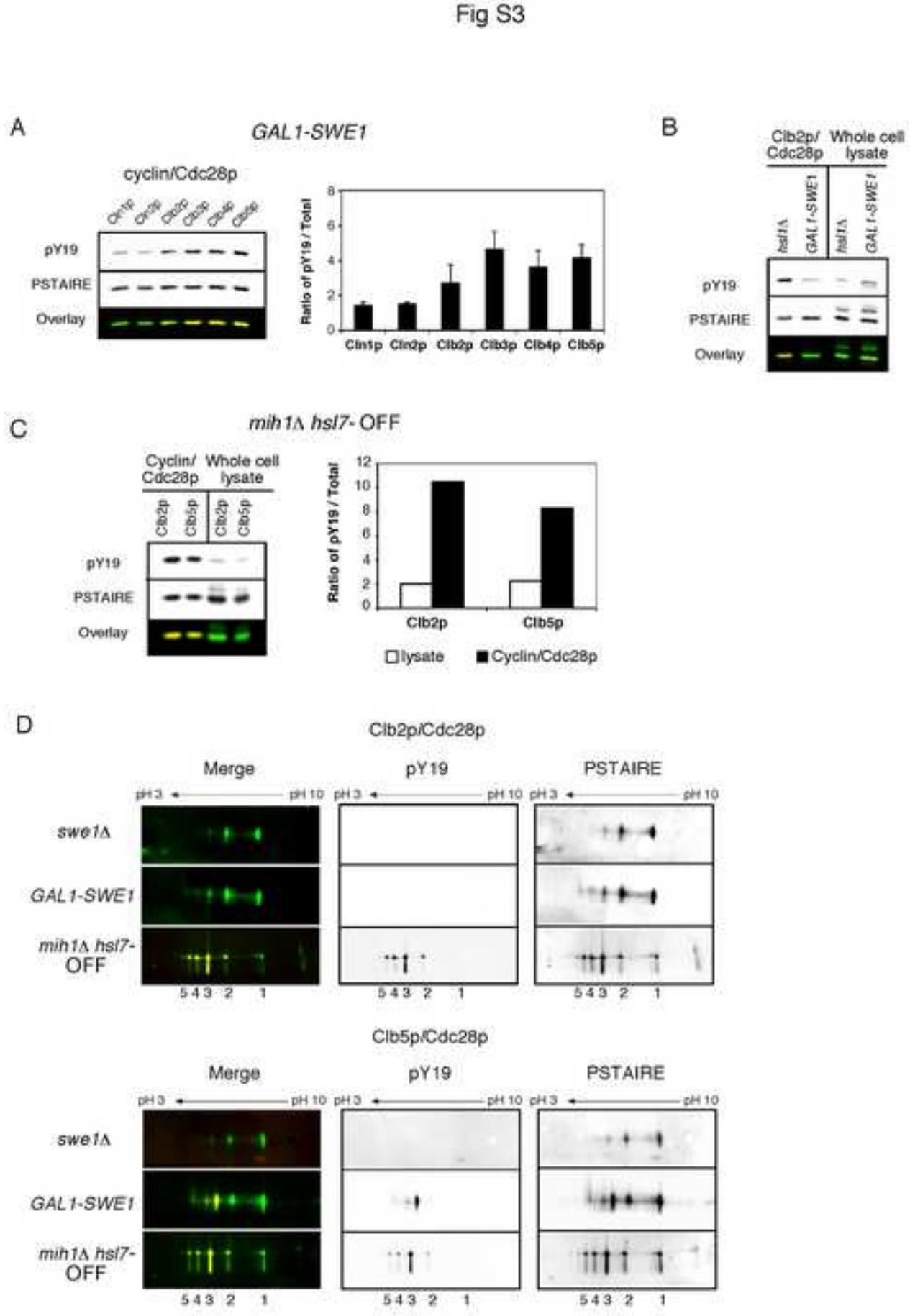
Fig S3
A
GAL1-SWE1
cyclin/Cdc28p
pY19
PSTAIRE
Overlay
Ratio of pY19 / Total
Cln1p Cln2p Clb2p Clb3p Clb4p Clb5p
B
Clb2p/ Cdc28p
Whole cell lysate
hsl1Δ
GAL1-SWE1
C
mih1Δ hsl7- OFF
Cyclin/ Cdc28p
Whole cell lysate
Clb2p
Clb5p
lysate
Cyclin/Cdc28p
D
Clb2p/Cdc28p
Merge
pY19
PSTAIRE
pH 3
pH 10
swe1Δ
GAL1-SWE1
mih1Δ hsl7- OFF
5 4 3 2 1
Clb5p/Cdc28p